Velocity and Attenuation of First Sound near the λ Point of Helium*

M. BARMATZ† AND I. RUDNICK
Physics Department, University of California, Los Angeles, California
(Received 15 December 1967)

The velocity and attenuation of first sound have been measured to within microdegrees of the λ transition of liquid helium at a frequency of 22 kc/sec. Relative sound-velocity measurements of 1 part in 10^6 could be obtained. The attenuation reaches a maximum about 1 or 2 μdeg below the transition while the velocity minimum occurs 6 μdeg below T_λ. Above the transition, the sound velocity satisfies the necessary condition for the validity of the Pippard-Buckingham-Fairbank relations out to at least 6 mdeg from the λ point. Below T_λ, the velocity shows an added temperature dependence beyond that expected from the Pippard-Buckingham-Fairbank relations, which is proportional to $|T_\lambda - T|^{0.9}$. If this temperature dependence persists, the velocity of sound above and below the transition approaches a common value of 217.3 m/sec at the λ point. Except in the immediate neighborhood of T_λ, the attenuation below the transition is proportional to $|T_\lambda - T|^{-1}$. This result is in agreement with the prediction of the Landau-Khalatnikov theory. Except in the immediate neighborhood of T_λ, the attenuation above the transition is proportional to $|T_\lambda - T|^{-1/2}$. This temperature dependence is not understood theoretically at present. Velocity dispersion results above and below the λ point are also presented.

I. INTRODUCTION

A. Pippard-Buckingham-Fairbank Relations

In a second-order phase transition the Ehrenfest relations govern the discontinuities in isobaric specific heat C_p, isobaric expansion coefficient β, and isothermal compressibility K_T:

$$\Delta C_p = \alpha V T \Delta\beta\,, \qquad \Delta\beta = \alpha \Delta K_T\,, \tag{1}$$

where V is the specific volume, T is the temperature, $\alpha = (dp/dT)_\lambda$ is the slope of the phase transition line, and the discontinuities are ΔC_p, $\Delta\beta$, and ΔK_T. A λ transition is characterized not only by the absence of a latent heat, and possible discontinuity in C_p, β, and K_T, but also by the fact that these quantities are singular, going to infinity as the λ transition is approached. Stronger conditions, the Pippard-Buckingham-Fairbank relations[1,2] (hereafter PBFR), govern these quantities in the immediate neighborhood of the λ transition, and can be written as follows:

$$C_p = \alpha V_\lambda T_\lambda \beta + C_0\,, \qquad \beta = \alpha K_T + \beta_0\,, \tag{2}$$

where

$$C_0 = T_\lambda \left(\frac{dS}{dT}\right)_\lambda, \quad \beta_0 = \frac{1}{V_\lambda}\left(\frac{dV}{dT}\right).$$

B. Simple Derivation of the PBFR

Consider a point on the entropy surface $S(p,T)$ of a substance and a line element through that point and lying on that surface. Then

$$\frac{dS}{dT} = \left(\frac{\partial S}{\partial T}\right)_p + \frac{dp}{dT}\left(\frac{\partial S}{\partial p}\right)_T. \tag{3}$$

Using the Helmholtz relation $\beta = -(1/V)(\partial S/\partial p)_T$ and the definition $C_p = T(\partial S/\partial T)_p$, one obtains

$$C_p = \left(\frac{dp}{dT}\right) V T \beta + T\frac{dS}{dT}\,, \tag{4}$$

where C_p, β, V, and T are the values at the point and dp/dT and dS/dT apply to the line element. This relation holds exactly at any point on the entropy surface, whether or not there is a λ transition. In particular it applies to the λ line. In the absence of infinite values of dp/dT and dS/dT it is clear that if C_p is singular, as it is at the λ line, so is β. If we consider points lying close to but not on the λ line, then, since C_p and β are singular, they will vary greatly for small displacements. There will be a small region where the variations of all qualities other than C_p and β can be neglected and thus the first PBFR is obtained. An exactly similar treatment applied to the volume surface $V(p,T)$ yields the second PBFR.

It is worthy of emphasis that if a transition is characterized by an absence of latent heat and a singularity in C_p then (a) there must also be a singularity in β and K_T and (b) there is no question that PBFR is exact in the limit. The only question has to do with the extent of the region around the λ line, where departures are insignificant.[3,4]

* Work supported in part by the U. S. Office of Naval Research.
† Present address: Bell Telephone Laboratories, Murray Hill, N. J.

[1] A. B. Pippard, Phil. Mag. **1**, 473 (1956).

[2] M. J. Buckingham and W. M. Fairbank, in *Progress in Low Temperature Physics*, edited by C. J. Gorter (North-Holland Publishing Co., Amsterdam, 1961), Vol. III, Chap. III.

[3] This is clearly pointed out in A. B. Pippard, *The Elements of Classical Thermodynamics* (Cambridge University Press, London, 1957), p. 145.

[4] K. C. Lee and R. D. Puff, Phys. Rev. **158**, 170 (1967).

C. Velocity of Sound at a λ Transition

It is not difficult to show that the low-frequency velocity u is given by the relation

$$\frac{V^2}{u^2}=-\left(\frac{\partial V}{\partial p}\right)_S=-\left(\frac{\partial^2 G}{\partial p^2}\right)_T+\left(\frac{\partial^2 G}{\partial p\partial T}\right)^2\left(\frac{\partial^2 G}{\partial T^2}\right)_p^{-1}, \quad (5)$$

where G is the Gibbs potential.

It is thus clear that in the Ehrenfest scheme of ordering phase transitions, depending as it does on the order of the derivative of the Gibbs potential which is discontinuous, the velocity of sound is in general discontinuous at first- and second-order phase transitions and is continuous at higher-order transitions. Furthermore, for λ transitions, the quantity u is continuous, as will be immediately evident, so that a sufficient condition that a transition be first or second order is the appearance of a discontinuity in the sound velocity. By use of PBFR and the relations

$$C_p=-T\left(\frac{\partial^2 G}{\partial T^2}\right)_p, \quad \beta=\frac{1}{V}\frac{\partial^2 G}{\partial p\partial T}, \quad K_T=-\frac{1}{V}\left(\frac{\partial^2 G}{\partial p^2}\right)_T,$$

it is not difficult to show by substitution in Eq. (5) that

$$\frac{2(u-u_\lambda)}{u_\lambda^3}\simeq\frac{1}{u_\lambda^2}-\frac{1}{u^2}=\frac{C_0^2}{\alpha^2V^2T}\frac{1}{C_p}, \quad (6)$$

where u_λ is the sound velocity at T_λ, and

$$u_\lambda^2=\alpha^2V^2T/(C_0-\alpha\beta_0VT). \quad (7)$$

It is thus seen that a necessary, but not sufficient, condition that PBFR hold is that the velocity of sound is a linear function of the reciprocal of the isobaric specific heat.

A measurement of the velocity of sound in the immediate neighborhood of the λ line will yield the following information:

(1) The region in which the necessary condition that PBFR is exact can be investigated by establishing the region in which the sound velocity and the reciprocal of the specific heat are linearly related.

(2) From the slope of u versus C_p^{-1} the quantity C_0/α, which is $(dS/dp)_\lambda$, can be determined.

(3) The velocity of sound at the λ line u_λ can be determined. Given an independent determination of C_0, Eqs. (6) and (7) can then be used to obtain β_0 and α.

In He-II near the λ transition, a relaxation phenomenon[5] results in acoustic attenuation and dispersion and, particularly because of dispersion, earlier measurements[6,7] could not be used in the way just described. For such purposes it is necessary to use low frequencies, and measurements at 9.75 kc/sec have recently been reported[8] where it was found that u and C_p^{-1} were linearly related in He-I but not in He-II. The He-II measurements were in the range 10^{-4} °K$<(T_\lambda-T)<10^{-2}$ °K. Moreover, the He-II sound-velocity data fit a simple power law in $(T_\lambda-T)$ which, if extrapolated (although as pointed out in Ref. 8, the validity of an extrapolation is questionable), lead to a sound-velocity discontinuity at T_λ. The purpose of the investigation reported here was to carry such measurements into the immediate neighborhood of the λ line with high precision.

The measurements were sufficiently accurate and the approach to the λ point sufficiently close that dispersion and attenuation effects were observable with reasonable precision in the microdegree region of the λ point even at these low frequencies. These results will also be reported.

II. EXPERIMENTAL METHOD

A. Apparatus

A standard glass double Dewar was used. The helium bath could be regulated to within ±0.001°K for extended periods of time. The bath temperature was measured by obtaining the vapor pressure with a Wallace and Tiernan FA 160 pressure gauge. Measurements of the sound velocity were made in a copper cylindrical resonator 4.4 cm long and 2.5 cm in diameter. The ends of the resonator were terminated with identical acoustic transducers which were of the solid dielectric condenser type.[9] The transducers were sealed to the resonator with indium seals. A cross section of the top transducer is shown in Fig. 1. A sheet of 0.00025-in.-thick Mylar,[10] aluminum coated on one side, was stretched across a solid copper back plate. The aluminized Mylar, which was grounded to the resonator body through the copper ring, acted as a movable plate of a parallel-plate capacitor. An ac voltage applied to the unbiased drive transducer produced sound waves of twice the impressed frequency. The pickup transducer was biased with 200 V dc and responded at the frequency of the sound propagating in the liquid. The top transducer had a storage volume above the back plate which was approximately 2% of the total volume of the resonator. The main purpose of this volume was to ensure that there was liquid helium between the two transducers without having liquid in the 0.013-in.-i.d. filling tube. Liquid in this tube would have introduced a variable hydrostatic pressure and superfluid heat leak. The bottom transducer was essentially identical to the top one except for the omission of the storage

[5] L. D. Landau and I. M. Khalatnikov, Dokl. Akad. Nauk SSSR **96**, 469 (1954).
[6] A. Van Itterbeck and G. Forrez, Physica **20**, 133 (1954).
[7] C. E. Chase, Phys. Fluids **1**, 193 (1958).
[8] I. Rudnick and K. A. Shapiro, Phys. Rev. Letters **15**, 386 (1965).
[9] W. Kuhl, G. R. Schodder, and F. K. Schröder, Acustica **4**, 519 (1954).
[10] Metalized Films, Hastings and Co., 2314 Market Street, Philadelphia, Pa.

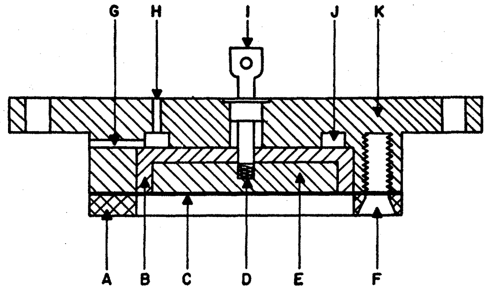

A. COPPER RING
B. NYLON INSULATOR
C. ALUMINUM FILMED MYLAR
D. SPRING FOR ELECTRICAL CONTACT
E. COPPER BACK PLATE
F. ONE OF SIX EQUALLY SPACED 2-56 SCREWS
G. ONE OF THREE FILLING PORTS TO RESONATOR
H. MAIN FILLING PORT
I. INCONEL - KOVAR ELECTRICAL FEEDTHROUGH
J. CIRCULAR RESERVOIR VOLUME
K. COPPER HOUSING

FIG. 1. Cross section of top transducer. The aluminized Mylar acts as a free vibrating plate of a parallel-plate capacitor.

volume and support tube. Each transducer could be used as a transmitter or receiver of sound.

The resonator was isolated from the surrounding He-II bath by placing it in a vacuum can. The 0.013-in.-i.d. stainless-steel capillary filling tube supported the resonator. A 2.3 kΩ heater (0.002-in.-diam Karma wire) was wound around the outside of the resonator. The current in the heater could be adjusted to balance the heat leak to the bath and small changes from this condition could be used to achieve controlled temperature drift rates. Helium gas from a storage volume kept at room temperature was condensed into the resonator. The sample chamber was initially cooled below the λ point using helium transfer gas in the vacuum can. The amount of helium transferred to the sample chamber could be determined by monitoring the initial and final pressures of the room-temperature storage volume using a Wallace and Tiernan FA 145 pressure gauge. Pressures could be read to within ±0.5 mm over the entire 0–1500-mm range of the gauge. After the transfer was completed, the gauge monitored the pressure in the resonator.

B. Temperature Measurements

The temperature of the helium in the sample chamber was measured with a Texas Instrument type 104A vented germanium thermometer. The resistor was placed along the axis of the resonator in direct contact with the liquid. Since the temperature range of this experiment was primarily ±25 mdeg about the λ point, calibrations using the usual three-constant Clement and Quinnel equation[11] were amply accurate. Owing to the poor thermal properties of He-I, all calibration points were taken below the λ point and the results extrapolated to the He-I range. The resistor had a λ-point value of 68 kΩ, at which temperature the sensitivity was 5 μdeg/Ω. The resistance was measured with an ac bridge system shown in Fig. 2. The phase-sensitive detector consisted of a transformer input audio amplifier with a gain of 10^7. The signal, after going through a mechanical chopper, was integrated and the dc output fed to a recorder.

In order to accurately measure temperature to within microdegrees of the λ point it was necessary to minimize self-heating in the resistor. For power inputs above 10^{-8} W, the self heating could be detected by a jump in resistance which occurred as the λ point was crossed. With input powers of 10^{-9} W or less, this jump no longer occurred.

In He-II the principal heat-transfer mechanism is normal-superfluid counterflow and there is excellent thermal equilibrium for nominal temperature drift rates. In He-I the principal mechanism is normal thermal convection and thermal equilibrium is adequate only where the expansion coefficient is appreciable and when the drift rate is quite slow. At $T-T_\lambda \simeq 6.3\times10^{-3}$ °K the expansion coefficient is zero and of different sign above and below this point. The convection reverses direction on drifting through this point and there is a characteristic thermal anomaly.

C. Velocity Measurements

The resonant frequencies of a cylindrical resonator are given by[12]

$$f=\tfrac{1}{2}u[(P/l)^2+(\alpha_{mn}/a)^2]^{1/2}, \quad (8)$$

where f is the resonant frequency, u is the sound velocity, P is zero or a positive integer, l and a are the length and radius, respectively, of the cylindrical enclosure, and α_{mn} is a solution of the relation

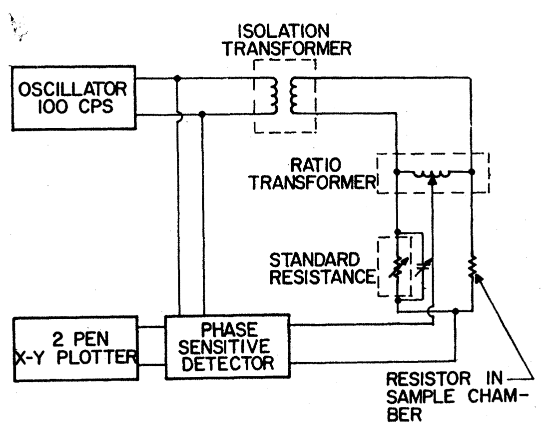

FIG. 2. ac resistance bridge.

[11] J. R. Clement and E. H. Quinnel, Rev. Sci. Instr. **23**, 213 (1952).

[12] P. M. Morse, *Vibration and Sound* (McGraw-Hill Book Co., New York, 1948), 2nd ed., p. 397.

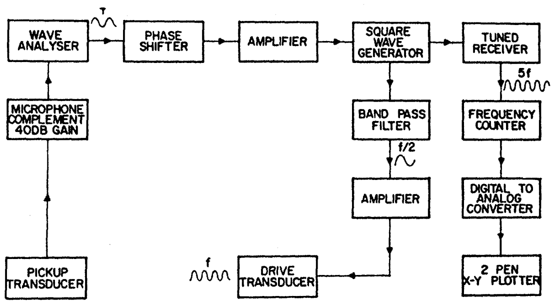

FIG. 3. Block diagram of transmitting and receiving system.

$d[J_m(\pi\alpha)]/d\alpha=0$, where $J_m(\pi\alpha)$ is a Bessel function of the first kind. The transducers used in this experiment have the property that they are best coupled to the plane-wave modes of the resonator which are characterized by $\alpha_{mn}=0$ and consequently the velocity is given by

$$u=2lf/P. \tag{9}$$

It was possible to continuously track a resonance as the sample chamber slowly drifted in temperature. The output of the pickup transducer was fed back to the drive transducer with sufficient gain and filtering to cause the circuit to self-oscillate at one of the plane-wave modes of the resonator (see Fig. 3). The wave analyzer was used in an afc mode which tracked the received signal f and also had an output of the same frequency. After passing through the phase shifter and amplifier the signal triggered a generator which produced a square wave whose period was twice that of the input sine wave. A bandpass filter, tuned to the first Fourier component of the square wave, produced a sinusoidal signal of frequency $\frac{1}{2}f$. The generator which halved the frequency was necessary since the frequency was doubled in converting the electrical signal to an acoustic signal at the drive transducer. The signal at the pickup transducer was amplified by 40 dB before returning to the wave analyzer input to complete the loop. Once the loop was self-oscillating the phase shifter was adjusted for a maximum input signal to the wave analyzer, which corresponded to the peak of the resonance. The system then self-oscillated at the resonant frequency of the resonator, as the temperature drifted, without further adjustment.

For the high Q modes of the resonator this self-oscillating technique gave stable frequency readings to better than 1 part in 10^5. High resolution was obtained by using a receiver tuned to one of the higher Fourier components of the square wave and feeding this signal to a counter. The binary-coded decimal (BCD) output of the counter corresponding to the last two digits was converted to a dc signal which was fed to a recorder.

The output of the square-wave generator was independent of input voltage. The change in amplitude of the acoustic signal as monitored on the input meter of the wave analyzer was then a measure of the change in quality factor Q of the resonator, which in turn is a function of the acoustic attenuation coefficient of the helium. Thus a record of the amplitude was used to determine the attenuation coefficient.

By using a two-pen recorder one could make simultaneous measurements of any two of the three quantities, velocity, attenuation, and temperature. Driving voltages of from 2 to 15 V rms were used during the experiments. Routine checks on the linearity of the system were made by doubling the input voltage. This produced no change in the resonant frequency to within the accuracy of adjusting the phase shifter, 1 or 2 parts in 10^5.

D. Calibration of Transducers; Magnitude of Temperature Swing in Sound Wave

An estimate of the temperature swing in the resonator produced by the acoustic sound wave was made using the relation which applies to the reciprocity calibration of transducers.[13] This relation for identical transducers is

$$M_0=[(V_2/I_1)(1/K)]^{1/2}, \tag{10}$$

where M_0 is the sensitivity of the transducer as a microphone in (esu of potential)/(dyn/cm^2). V_2 and I_1 are, respectively, the microphone open-circuit potential difference and the driver current in esu. The four-terminal network is shown in Fig. 4. K is the ratio of the pressure P_2 (dyn/cm^2) at the microphone face to the volume velocity (cm^3/sec) at the driver and depends on the acoustic geometry. If u_1 is the particle velocity at the driven face (cm/sec) and S (cm^2) is the area of the transducer, K is given by

$$K=P_2/Su_1. \tag{11}$$

When the frequency of the driver corresponds to a natural frequency of the resonator a standing wave is set up between the transducers. If the pressure amplitude in the forward-going wave is P_0 and the attenuation in the medium is α (Np/cm) then the pressure at the microphone face is $P_2=2P_0e^{-\alpha l}$. The velocity at the driver face due to the interference of the forward-going

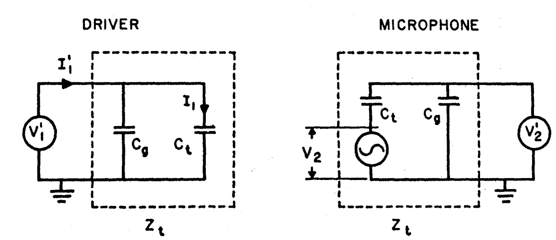

FIG. 4. Four-terminal reciprocity network. C_t: capacitance of a transducer. C_g: cable capacitance. Z_d: combined impedance of a transducer and cable. V_2: generated microphone voltage. V_2': measured microphone voltage. I_1: actual driving current. I_1': measured driving current. V_1': measured driving voltage.

[13] W. R. Maclean, J. Acoust. Soc. Am. 12, 140 (1940).

and reflected plane waves is $u_1=(P_0/\rho u)(1-e^{-2\alpha l})$. For the case $\alpha l \ll 1$,

$$K=(2\rho u^2/Sl\omega)Q. \tag{12}$$

Defining the driver and microphone units to consist of a transducer and its respective cables leads to a maximum pressure in the standing wave given by

$$P_2=\left(\frac{V_1'V_2'}{Z_T}\frac{2\rho u^2 Q}{Sl\omega}\right)^{1/2}\times 10^{7/2}, \tag{13}$$

where now V_1' and V_2' are expressed in volts and Z_t is the impedance in ohms of the microphone-cable system. The capacitance of the cables and transducer was approximately 350 pf. At the frequency of 22 kc/sec the Q of the resonator was approximately 400 at T_λ. V_1' never exceeded 15 V and usually was considerably smaller; at this maximum value V_2' was approximately 3×10^{-5} V. The maximum pressure, using these values, is 57 dyn/cm². At low frequencies, sound is propagated under isentropic conditions. The ratio of the pressure swing to the temperature swing is given by $(\partial p/\partial T)_S=C_p/TV\beta$. At 10^{-6} °K from the λ point this gives $(\partial p/\partial T)_S\simeq 1.40\times10^8$ dyn/cm² °K, resulting in a maximum temperature swing in the resonator of 4×10^{-7} °K, which is beyond the temperature resolution of the experiment.

III. RESULTS

A. Presentation and Interpretation of Data

The velocity of sound has been measured within ±20 mdeg of the λ transition using the techniques described in the previous section. A slow drift through the transition is shown in Fig. 5. The resonant frequency of the ninth harmonic (22 kc/sec) and the output amplitude are recorded simultaneously as a function of time. The spike marks on the amplitude curve record the times at which the resistance bridge was balanced, and therefore the temperature was known. The anomalous behavior of the velocity and attenuation of sound near the transition can clearly be seen. The smallest steps in the frequency curve corresponded to relative velocity changes of less than one part in 10^5. It is apparent that the velocity of sound minimum and attenuation maximum do not occur at the same temperature. The temperature of the attenuation maximum is very near that of an inflection point of the velocity curve. The minimum in velocity and maximum in attenuation were separated by approximately 4 μdeg at this frequency.

The position of the λ point was determined by the difference in heat transfer in He-I and He-II. Figure 6 shows the resonant frequency and resistance with constant heat input as a function of time for an 8-min period, during which the temperature drifted up 80 μdeg. Because of the excellent heat transfer by the superfluid, the resonator walls, liquid, and resistor are in thermal equilibrium at all temperatures below T_λ ($a\rightarrow b$). However, upon crossing the transition, this mode of heat transfer ceases and the principal heat-transfer mechanism is thermal convection. Convection can be pronounced in the neighborhood of the λ point because of the large thermal-expansion coefficient of He-I. Since the circulating convective currents take time to be established, there is a period during which the resistor shows no change in temperature ($b\rightarrow c$). When the warm liquid sinks along the walls and finally rises along the axis there is a sudden increase in the temperature of the resistor (d). When the convective flow reaches a steady state, the liquid and resistor are once again in good thermal equilibrium. The λ point is at the intersection of ab and bc and within an uncertainty of a microdegree or two occurs at the inflection point of the velocity curve. Thus, the attenuation maximum occurs very close to the λ point and the velocity of sound minimum is about 4 μdeg lower. Later in this paper we present evidence that the attenuation maximum actually occurs 1.8 μdeg below the λ point.

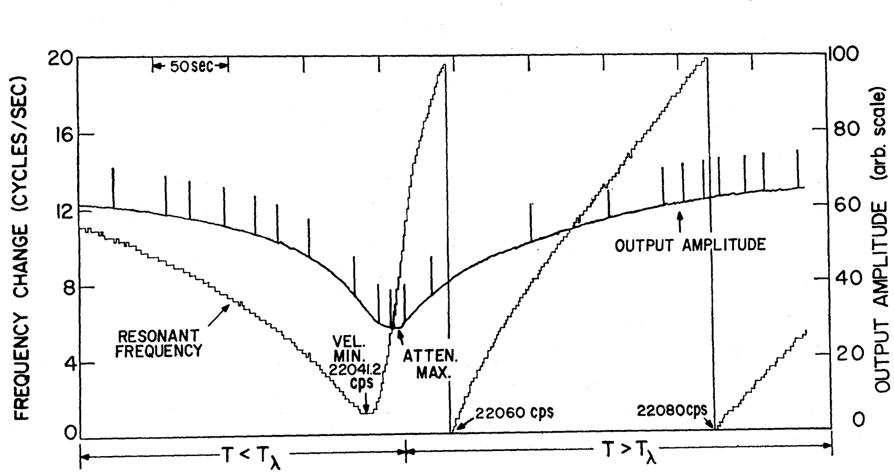

FIG. 5. Sound velocity and attenuation in the neighborhood of the λ point. These measurements cover the temperature range from 40×10^{-6} °K below to 75×10^{-6}°K above the transition. The smallest steps in the frequency curve correspond to relative velocity changes of less than 1 part in 10^5 and a reregistry occurs every time 100 such steps accumulate.

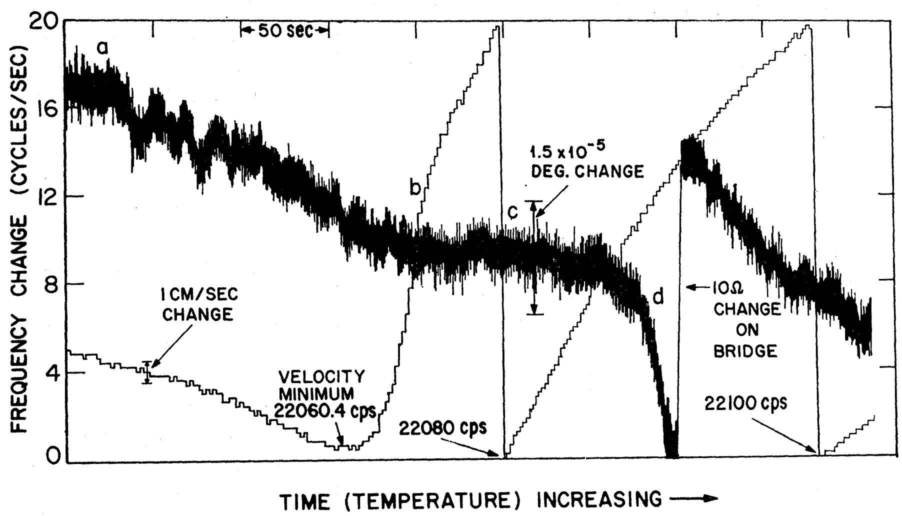

FIG. 6. Simultaneous measurement of temperature and frequency. It is characteristic that there is a break in the heating curve on crossing the λ point. The slope becomes small until the convection current is established at *d*, where there is a sharp increase in temperature along the axis of the resonator followed by a normal heating curve.

B. Sound Velocity Measurements from 1.8 to 2.5°K

For purposes of comparison, the temperature dependence of the sound velocity was determined in an extended region about the λ point. Figure 7 shows velocity measurements from 1.8 to 2.5°K. Measurements of Chase[7] and Van Itterbeek and Forrez[6] are also shown. Chase used a pulse technique to measure the velocity at 1 Mc/sec while Van Itterbeek and Forrez used an acoustic interferometer in the frequency range 200 to 800 kc/sec. The temperatures used in the earlier investigations, which referred to the 1948 He^4 vapor-pressure scale,[14] have been adjusted to fit the 1958 He^4 temperature scale. The data of the present investigation agree quite well with the earlier measurements and has smaller scatter.

C. Velocity of Sound near T_λ

The temperature dependence of the velocity within 20 mdeg of the λ transition is shown in Fig. 8. The total change of the velocity within this region is only 1%. The anomaly at about 6 mdeg above the transition occurs at the temperature of the density maximum. The anomalous behavior is not in the sound velocity, which is smoothly varying in this region, but in the tempera-

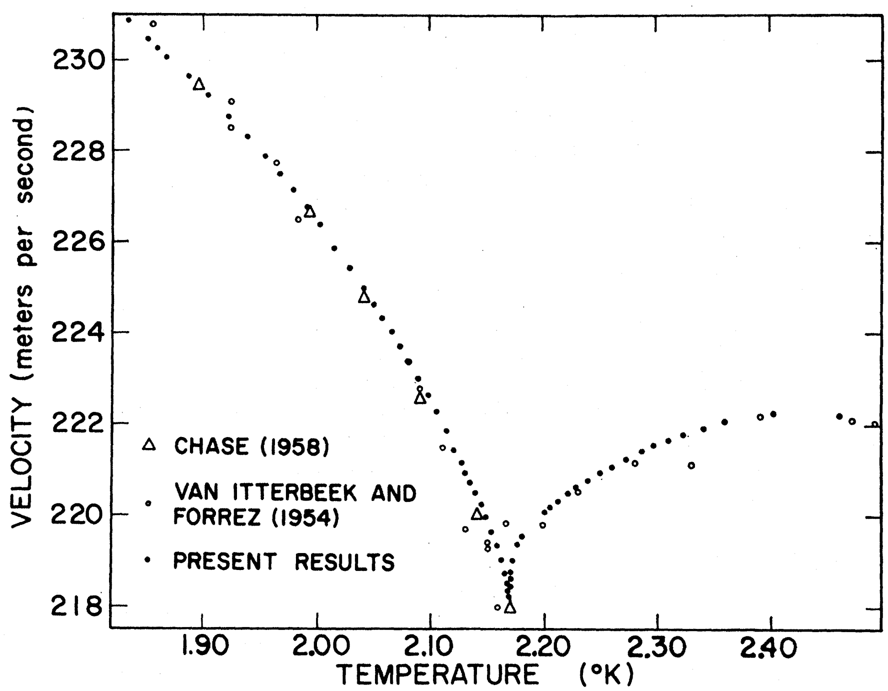

FIG. 7. Temperature dependence of the sound velocity in an extended region about the λ point.

[14] H. van Dijk and D. Shoenberg, Nature **164**, 151 (1949).

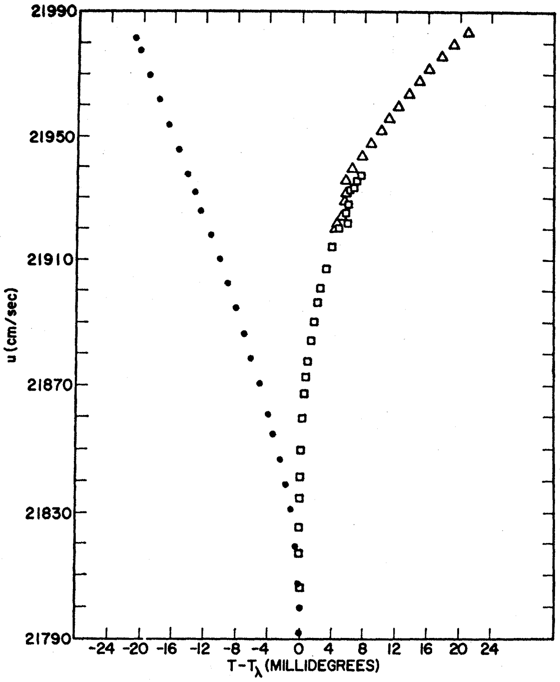

FIG. 8. Temperature dependence of the sound velocity within ±20 mdeg of the transition. The data designated by ● and □ were taken at the same time during a slow drift upward in temperature. An anomaly in the temperature measurement occurs above the transition at the density maximum.

ture measurement and is caused by the reversal of the convective current, as discussed previously. The temperature of the density maximum can be determined using this convective anomaly and is found to be $T_\lambda+0.00628\pm0.0001$°K. Details will be given in a separate paper. Figure 9 shows the temperature dependence of the velocity in regions successively closer to the λ point. The anomaly in the sound velocity at T_λ is apparent on each of the three scales.

In Fig. 10 the velocity is plotted against the reciprocal of C_p, using specific-heat values calculated from the Buckingham and Fairbank relation[2]

$$C_p=4.55-3.00\log_{10}|T-T_\lambda|-5.20\Delta\ (J/g°K)\,, \quad (14)$$

where $\Delta=0$ for $T<T_\lambda$ and $\Delta=1$ for $T>T_\lambda$. The velocity u is taken with respect to $u_{\min}$, the minimum value measured experimentally. Since there was some question about the quality of the thermal equilibrium in He I during a drift, some measurements were made under equilibrium conditions and are shown by crosses. These agree well with those taken while drifting.

The necessary condition that PBFR hold is satisfied above the λ point, where a linear relationship extends at least out to 6 mdeg. A least-squares fit to the equation

$$u_{\rm I}-u_{\min}=A/C_p+B \quad (15)$$

out to 3 mdeg gave

$$A=12.0\times10^9\ ({\rm cgs}, °{\rm K}) \quad {\rm and} \quad B=-58.6\ {\rm cm/sec}. \quad (16)$$

Below the λ point, there are serious departures from the linear relationship for temperatures greater than a millidegree from the transition. In the range $T_\lambda-T$ somewhat less than a millidegree, the points appear to lie along the line determined by the He-I data. This departure does not necessarily imply that the PBFR are invalid below the transition. As has been shown, small systematic deviations of k_T, C_p, or β from the limiting logarithmic behavior[8] or a small temperature dependence of c_0 or β_0[15] could account for the observed temperature dependence of the sound velocity. The velocity is a sensitive parameter for measuring departures from the PBFR. There is an important difference between the present results and the earlier work of Rudnick and Shapiro.[8] The earlier investigation found a 0.1% shift in velocity between the He-I and He-II curves of Fig. 10. This shift is unexplained but may be caused by an end correction which underwent a jump at the transition. In any case these results supersede those. As was found in the earlier work, the present data below the transition can be fitted over three decades in $(T_\lambda-T)$ with a relation of the form

$$(u_{\rm II}-u_{\min})=D(T_\lambda-T)^{1/2}. \quad (17)$$

An extrapolation of this temperature dependence to the transition is very questionable,[8] but it is clear that if this is done $u_{\min}$ is the velocity at the λ point and is approximately 60 cm/sec greater than the λ point velocity found from the He-I data. It has been shown[16]

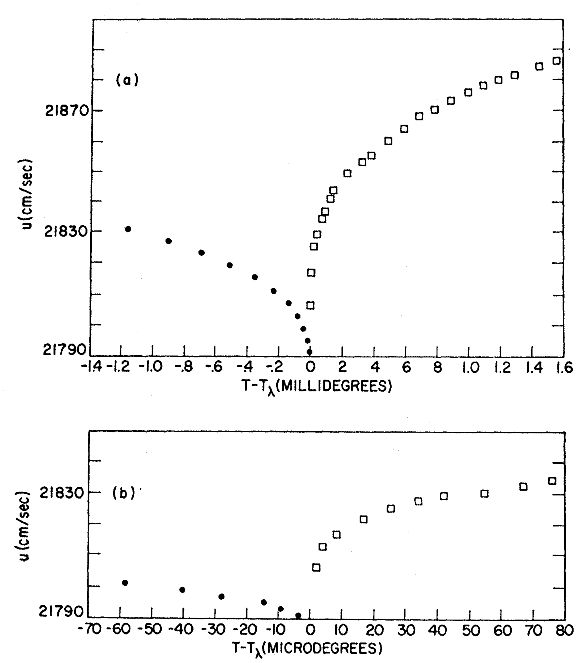

FIG. 9. Sound velocity in temperature regions successively closer to the transition. These measurements were made at a frequency of 22 kc/sec while drifting slowly up in temperature.

[15] D. H. Douglass, Jr., Phys. Rev. Letters 15, 951 (1965).

[16] M. Revzen, A. Ron, and I. Rudnick, Phys. Rev. Letters 15, 384 (1965).

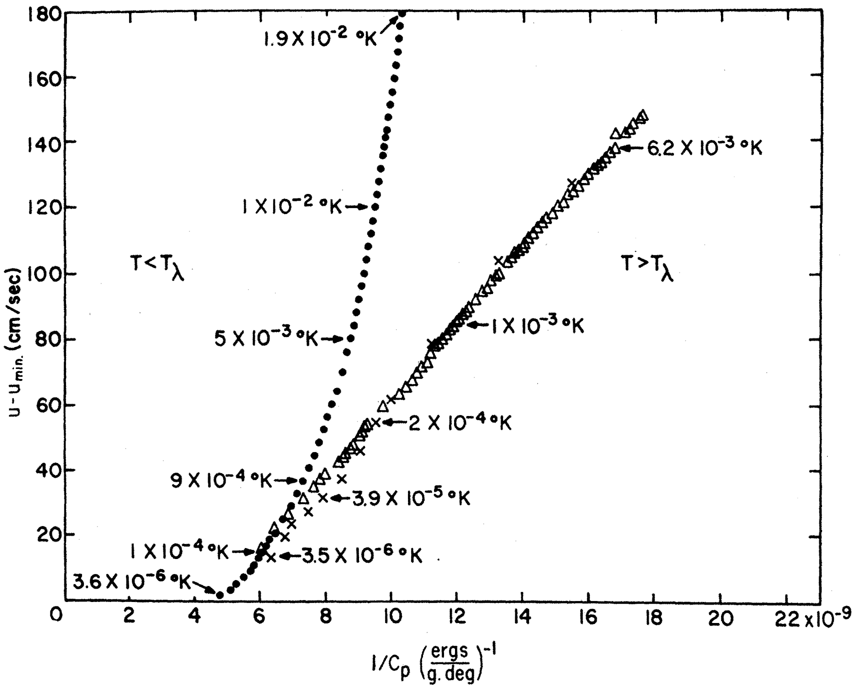

FIG. 10. Measurement of the velocity difference $u-u_{\min}$ against $(C_p)^{-1}$. $u_{\min}$ is the minimum measured velocity. ● and △—steady drift up in temperature. ×—measurements under equilibrium situation. As the transition is approached within microdegrees the curves above and below T_λ overlap and lie along the line determined by the He-I data.

that a discontinuity in velocity implies the existence of two λ lines with slightly different slopes, which in turn implies a narrow intermediate state at higher pressures.

The velocity below the transition can be written in the following form, which does not introduce a velocity discontinuity:

$$u_{\mathrm{II}}-u_{\min}=A/C_p+B+D|\Delta T|^n. \tag{18}$$

The exponent n is dependent on the choice of the constants A and B. These constants, in turn, depend on the extent of the temperature region from which data is used in their determination. Figure 11 shows the temperature dependence of the excess velocity $u_{\mathrm{II}}-u_{\mathrm{I}}$ at a given value of C_p. This is the difference between the sound velocities on the two sides of the transition at a given abscissa in Fig. 10. The best-fit values of the constants A and B for data in the range 2×10^{-2} °K below to 3×10^{-3} °K above the transition were used in this plot. A comparison of the two relations, Eqs. (17) and (18), with the present data and the earlier work[8] is shown in Fig. 12. With the increased resolution of the present experiment, small systematic deviations from the square-root relation can be seen. Equation (18) appears to give a better fit to the present

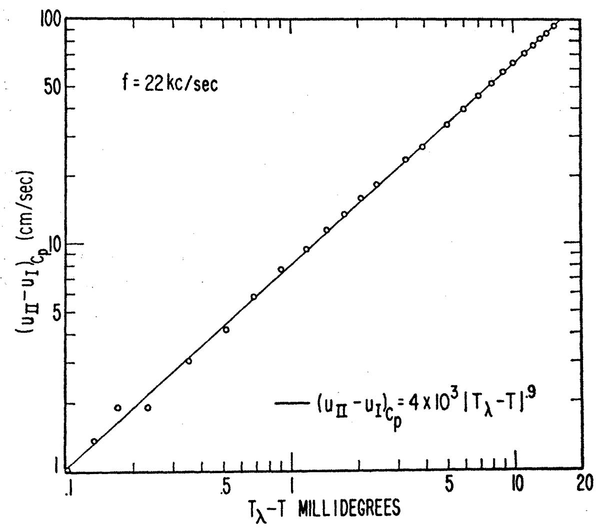

FIG. 11. Temperature dependence of the excess velocity. The data points correspond to using $A=12.0\times10^{9}$ (cgs, °K) and $B=-58.3$ cm/sec in Eq. (18).

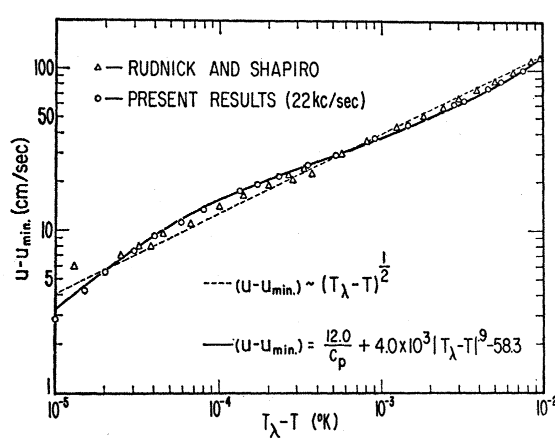

FIG. 12. Comparison of Eqs. (17) and (18) with the velocity below the transition.

data, although it must be emphasized that basically discrepancies in the velocity of less than a few parts in 10^5 are involved in making this judgment.

The asymmetry of the fit to PBFR above and below T_λ is reminiscent of a similar asymmetry in the average value of the order parameter in the Landau theory of second-order phase changes[17] which takes on nonzero values only below the transition. While at first glance this would appear to be a promising avenue of exploration, there are basic difficulties. The Landau theory applies to second-order phase changes which we have shown are characterized by a sound-velocity discontinuity, whereas the liquid-helium phase change is a λ transition where no such discontinuity is expected. To a certain extent this difficulty can be avoided by incorporating, in the order-parameter–independent part of the Gibbs function, a temperature dependence which is appropriate to a λ transition. A difficulty remains, however, that the usual Landau expansions are not carried out to high enough order to yield the temperature dependence of the second derivatives of the Gibbs function, which is necessary in obtaining the temperature-dependent velocity. When, in fact, the expansions are carried out to higher orders it is possible to show that below the λ point there is an added temperature-dependent term which to lowest order is proportional to $(T_\lambda - T)$, not unlike the last term in Eq. (18). A recent phenomenological theory of the λ transition[4] also leads to a similar added temperature-dependent term in the velocity. However, it is not possible to determine the magnitude of this term on the basis of other independent data. For this purpose one would require highly accurate measurements of C_p, β, and K_T in the immediate neighborhood of T_λ in He II.

The best-fit values of the exponent n and coefficients found from this experiment from 2×10^{-2} °K below to 3×10^{-3} °K above T_λ are

$$n=0.9\,,\quad A=12.0\times10^9\ (\text{cgs, °K})\,,\quad B=-58.3\ \text{cm/sec}\,, \tag{19}$$

and

$$D=4\times10^3\ (\text{cgs, °K})\,.$$

From the results of this experiment, values of the Pippard constants α, C_0, and β_0 have been found. C_0 is determined by locating the temperature at which $\beta=0$, at which point $C_p=C_0$, and using the value of C_p in Ref. 2. β_0 and α are determined from u_λ and the value of A using Eqs. (6) and (7). $(dS/dp)_\lambda$ has also been determined. These quantities are compared with the results of other observers in Table I. In the vicinity of the λ point the PBFR take the form

$$C_p=1.82\times10^2\beta+5.97\ (\text{J/g °K})\,,\quad \beta=1.22\times10^8K_T+1.74\ (\text{°K})^{-1}\,. \tag{20}$$

Of particular interest is the slope of the λ line. The present determination has the disadvantage that it is indirect. Direct determinations face the difficulty that the slope is a rapidly changing function of pressure at the vapor pressure, and consequently highly accurate determinations of temperature and pressure close to this point are necessary. Thus, the determination of the slope, at a point, as in the present instance, has a real advantage.

D. Attenuation of Sound

Besides the anomalous behavior in the sound velocity, there is attenuation and dispersion close to the λ point. Pellam and Squire[18] were the first to observe a large attenuation near the transition. Measurements by Chase[7] at a frequency of 1 Mc/sec showed a velocity of sound minimum below the transition and an attenuation maximum between the λ point and the velocity minimum. When dynamic processes occur near the λ point the reestablishment of equilibrium takes place comparatively slowly. By associating a relaxation time τ with these processes, it has been shown[19] that the sound velocity is given by

$$u^2=\frac{1}{(1-i\omega\tau)}[u_0^2-i\omega\tau u_\infty^2]\,, \tag{21}$$

where u_0 and u_∞ are, respectively, the sound velocities in the low- and high-frequency limits. Under the condition $\chi=(u_\infty-u_0)/u_0\ll1$, the velocity and attenuation associated with this relaxation mechanism can be written in the form

$$u=u_0\left(1+\chi\frac{\omega^2\tau^2}{1+\omega^2\tau^2}\right) \tag{22}$$

and

$$\alpha=\frac{\chi}{u_\infty}\left(\frac{\omega^2\tau}{1+\omega^2\tau^2}\right). \tag{23}$$

A complication in applying this in the present instance is that experimentally u_0 is strongly temperature-dependent near T_λ. This is a direct consequence of the fact that the framework for the theory is that of a second-order phase transition (where no such strong temperature dependence obtrudes) while the real situation is that of the λ transition. The two are rendered compatible by allowing u_0 and u_∞ to be strongly temperature-dependent but their difference to be constant.

The Q of a resonant system is given by $Q=2\pi E_s/E_L$, where E_s is the energy stored and E_L is the energy lost per cycle. E_s is proportional to the square of the amplitude A of the sound in the resonator, while E_L is

[17] L. D. Landau, Physik Z. Sowjetunion **11**, 26 (1937); **11**, 545 (1937); L. D. Landau and E. M. Lifshitz, *Statistical Physics* (Addison-Wesley Publishing Co., Reading, Mass., 1958), Chap. 14.

[18] J. R. Pellam and C. R. Squire, Phys. Rev. **72**, 1248 (1947).

[19] L. D. Landau and E. M. Lifshitz, *Fluid Mechanics* (Addison-Wesley Publishing Co., Reading, Mass. 1959), p. 304.

TABLE I. Comparison of thermodynamic quantities at the λ point.

	α (atm °K^{-1})	β_O (°K^{-1})	C_O (J g^{-1} °K^{-1})	$(dS/dp)_\lambda$ (J atm^{-1} g^{-1} °K^{-1})	u_λ (m/sec)
Present work	−120	1.74	5.97	-2.25×10^{-2}	217.3
Buckingham and Fairbank[a]	−130	1.9		-1.77×10^{-2}	216.0
Rudnick and Shapiro[b]	−129	1.85		-2.25×10^{-2}	218.2[c]
					219.0[d]
Chase, Maxwell, and Millett[e]	− 97.5	1.378	6.3		
Kerr and Taylor[f]	−118.4		6.38$T>T_\lambda$		
			5.34$T<T_\lambda$		
Lounasmaa and Kaunisto[g]	− 98	1.223			
Chase[h]					218.0
Elwell and Meyer[i]	−114	1.66			
Kierstead[j]	−111.1	1.60			
Ahlers[k]	−114				

[a] Reference 2.
[b] Reference 8.
[c] Limiting value as the transition is approached from above.
[d] Limiting value as the transition is approached from below.
[e] C. E. Chase, E. Maxwell, and W. E. Millett, Physica **27**, 1129 (1961).
[f] E. C. Kerr and R. D. Taylor, Ann. Phys. (N. Y.) **26**, 292 (1964).
[g] O. V. Lounasmaa and L. Kaunisto, Ann. Acad. Sci. Fennicae, Ser. A VI, No. **59** (1960).
[h] Reference 7.
[i] D. Elwell and H. Meyer, Phys. Rev. **164**, 245 (1967).
[j] H. A. Kierstead, Phys. Rev. **162**, 153 (1967).
[k] G. Ahlers, Bull. Am. Phys. Soc. **12**, 1063 (1967); and (private communication).

proportional to u_1^2R, where R is the acoustic resistance and u_1 is the velocity of the Mylar membrane. If the transducer has a high mechanical impedance then u_1 will be independent of the acoustic load. Far from the transition, the acoustic resistance at the source is due primarily to the background attenuation. Under these assumptions $Q\sim A^2$ and the attenuation α in Np/cm, is[20]

$$\alpha=\omega/2Qu\sim1/A^2. \tag{24}$$

The acoustic conditions throughout the temperature range are demonstrably not those used in obtaining this equation, and in the absence of certain knowledge about them recourse to experiment was necessary. The shape and peak height of the resonant tuning curve was obtained using a very stable sweep oscillator. Interestingly enough it was found that $Q\sim A^2$ within experimental error both above and below the λ point to within 10^{-5} °K of the transition. During the actual experiment the Q of the resonator was also measured using the relation $Q=f/(f_2-f_1)$, where f_2 and f_1 are the half-power frequencies. The absolute value of the attenuation was determined by averaging the Q's obtained from the tuning-curve measurements and the half-power frequency method. The absolute accuracy of the attenuation measurements was about 15%; the relative values are considerably more accurate.

Because of the lag in establishment of thermal equilibrium just above the λ point, an alternative method had to be employed to measure temperatures in the microdegree neighborhood of the transition. Measurements close to the transition were made with a constant heat input. The power input to the resonator was determined from the temperature drift rate below the transition. Using the known temperature dependence of the specific heat,[2] the temperature departure from T_λ could then be determined from time difference measurements.

The attenuation measured at a frequency of 22 kc/sec is shown in Fig. 13. There was a background attenuation which amounted to about 20% of the maximum attenuation measured. Below T_λ there is good agreement to within 1.5×10^{-5} °K of the transition between

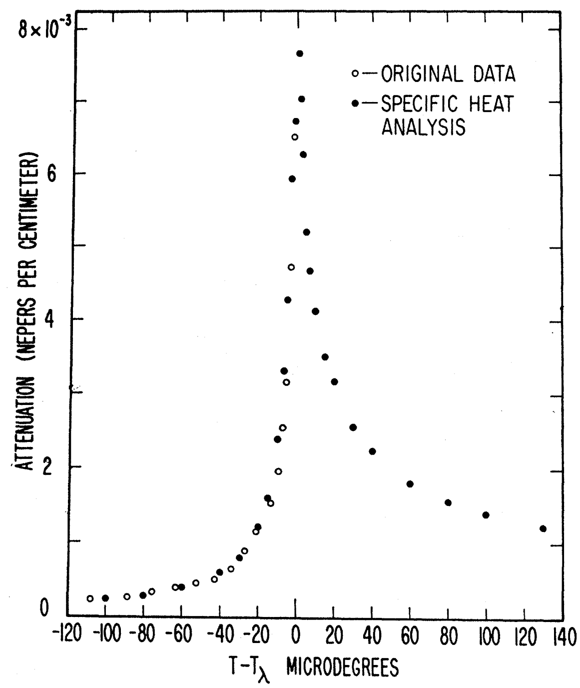

FIG. 13. Temperature dependence of attenuation at 22 kc/sec. This data has been corrected for background attenuation.

[20] Close to the transition the acoustic resistance is due primarily to the attenuation in the medium. This could then lead to $Q\sim A$ and $\alpha\sim1/A$.

the actual temperature measured experimentally and the temperature calculated from the specific-heat temperature dependence. In the limit $\omega\tau \ll 1$, the attenuation relation Eq. 23 reduces to

$$\alpha = (\chi/u_\infty)\omega^2\tau. \tag{25}$$

The temperature dependence of the attenuation is the same as the relaxation time in the lim$\omega\tau \ll 1$, since frequency changes can be considered negligible.

1. He-II

Landau and Khalatnikov[5] (hereafter LK) have treated the problem of attenuation near a second-order phase transition. In the case of helium the establishment of equilibrium between the normal and superfluid components proceeds extremely slowly just below the λ point. This process can be characterized by the relaxation of the order parameter to its equilibrium value. The classical approach to phenomena near critical points developed by Landau[17] leads to a relaxation time for $T < T_\lambda$ of the form

$$\tau = \frac{D}{|T - T_\lambda|}, \tag{26}$$

where D is a constant. Since the expectation value of the order parameter is zero above the transition, this theory makes no prediction above the λ point.

Figure 14 is a plot of total measured attenuation (including background) versus $|T_\lambda - T|^{-1}$ for measurements above and below the transition. Except in the immediate neighborhood of the transition, the data below T_λ fall along a straight line and thus have the temperature dependence predicted by the LK theory. This has also been observed by Chase[7] for frequencies in the megacycle region. The ratio of the absolute values of attenuation at 22 kc/sec and 1 Mc/sec is proportional to the ratio of the frequencies to the 1.9 power for the attenuation below T_λ. The attenuation above T_λ is definitely not proportional to $|T_\lambda - T|^{-1}$.

Equation (23) can be rewritten in the form

$$\alpha/\omega = H(Z), \quad H(Z) = \frac{\chi}{u_\infty}\frac{Z}{Z^2+1}, \tag{27}$$

where $Z = \omega\tau$. The function $H(Z)$ is logarithmically symmetric about $Z = 1$, where the attenuation reaches a maximum. Comparing the attenuation data at 22 kc/sec with the function $H(Z)$ yields the temperature at which $\omega\tau = 1$, the strength of the attenuation, χ/u_∞, and leads to the following values of the constants in the LK theory: $u_\infty - u_0 = 47$ cm/sec and $D = 1.3\times10^{-11}$ sec °K. This value of D, which corresponds to $\omega\tau = 1$ at $T_\lambda - T = 1.8\times10^{-6}$ °K, is also consistent with data obtained at 44 kc/sec.

In order to correlate the effects of attenuation, dispersion, and velocity near the transition, measurements were made with the system simultaneously self-oscillating at two resonant frequencies. These measurements were possible because of the rather flat response

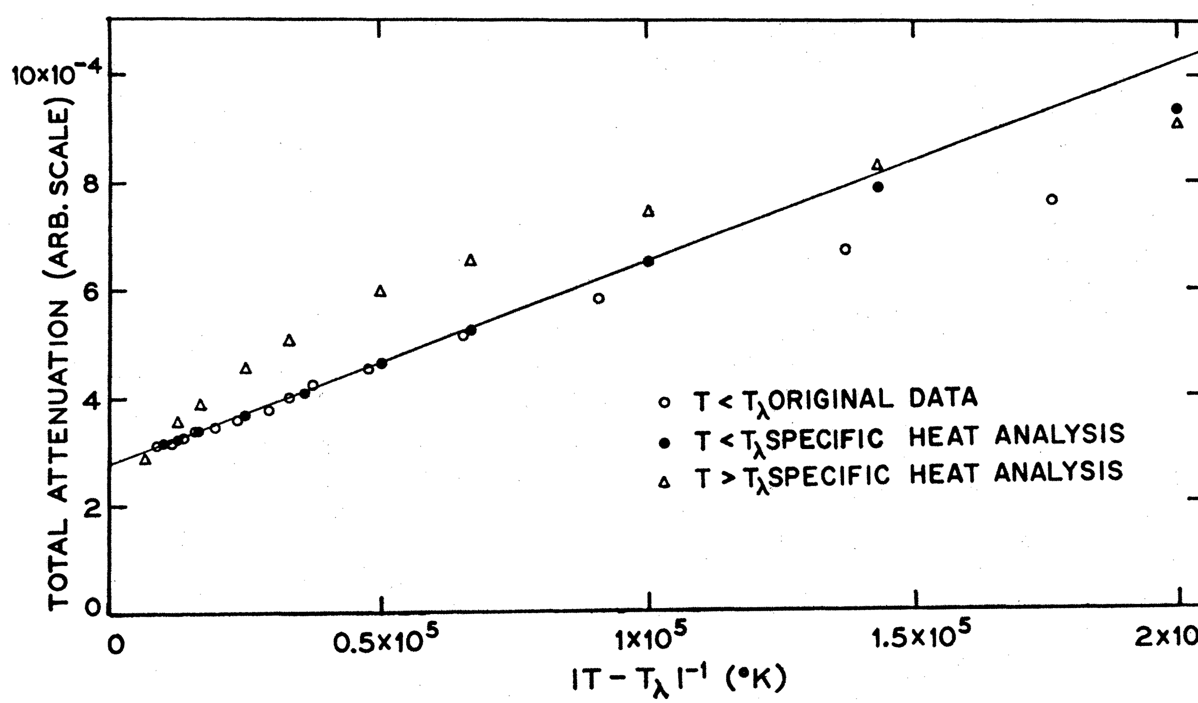

FIG. 14. Total attenuation (arb. scale) versus $|T - T_\lambda|^{-1}$ °K. The vertical intercept of the solid line gives the background attenuation below the 5 point.

of the capacitive transducers over the frequency range 1 to 100 kc/sec. Two electronic systems similar to that shown in Fig. 3 were locked to the seventh and eighteenth harmonics. These simultaneous data obtained from a pair of two pen X-Y recorders are shown in Fig. 15. By monitoring the ratio of the resonant frequencies, the position of the dispersion maximum relative to the other extrema could clearly be seen. The temperature dependence of the dispersion is shown in Fig. 16.

Equations (22) and (23) predict the dispersion maximum to occur below the transition. For angular frequencies of ω_1 and ω_2 the position of the dispersion

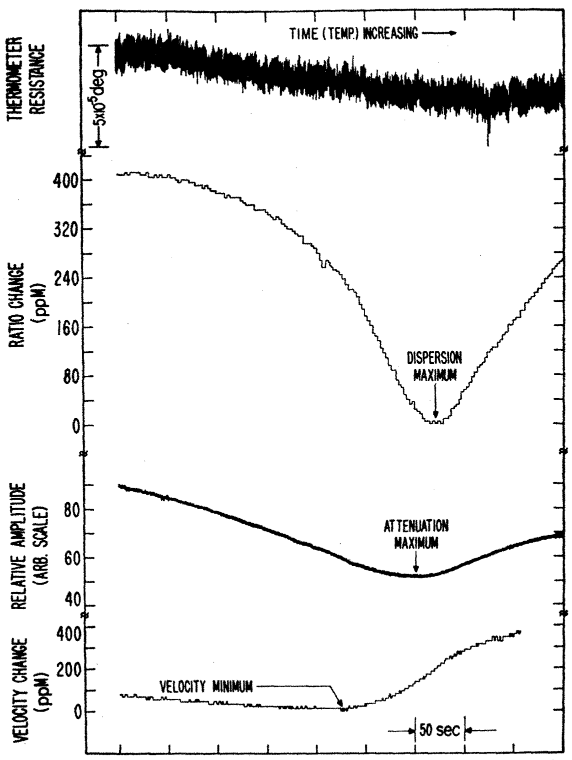

FIG. 15. Simultaneous measurement of temperature, dispersion, attenuation, and velocity. The attenuation and velocity correspond to the 44-kc/sec resonance. The dispersion is the ratio of 6.5 times the frequency of the seventh harmonic to the frequency of the eighteenth harmonic.

maximum is given by the relation $\tau^2=1/\omega_1\omega_2$ and has the value

$$(u_2-u_1)_{\max}=(u_\infty-u_0)\left(\frac{\omega_2-\omega_1}{\omega_2+\omega_1}\right). \tag{28}$$

The general relation for dispersion can be written in the form

$$u_2-u_1=(u_\infty-u_0)F(Z,\omega_1/\omega_2), \tag{29}$$

where

$$F(Z,\omega_1/\omega_2) =[1-(\omega_1/\omega_2)^2]\left(\frac{Z^2}{(1+Z^2)[1+(\omega_1/\omega_2)^2Z^2]}\right). \tag{30}$$

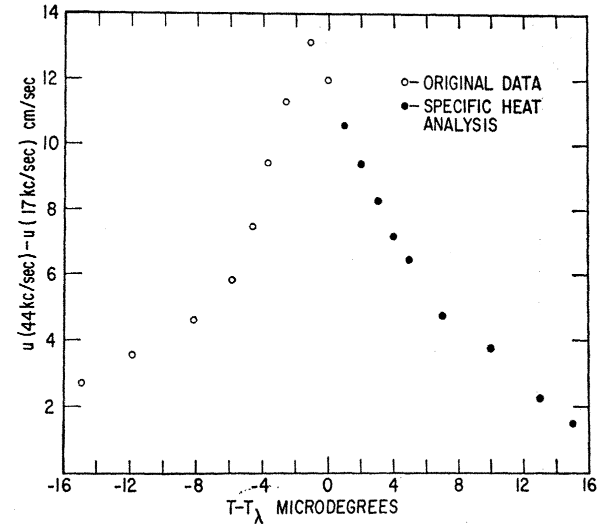

FIG. 16. Temperature dependence of dispersion.

A comparison of the dispersion between the seventh and eighteenth harmonics with the function $F(Z,\omega_1/\omega_2)$ gives the following values for the constants of the LK theory: $u_\infty-u_0=22$ cm/sec and $D=2.04\times10^{-11}$ sec °K.

It can be shown that T_λ, T_α (the temperature of maximum attenuation), and T_D (the temperature of maximum dispersion) are related in the following way:

$$T_\lambda-T_\alpha=\frac{T_D-T_\alpha}{[1-(\omega_1/\omega_2)^{1/2}]}. \tag{31}$$

At the frequencies used in this experiment the temperature difference between the maxima was only a few microdegrees and thus subject to large uncertainties. Values of $u_\infty-u_0$ and D determined from these temperature differences are in qualitative agreement with those found by the other methods above. A more accurate determination of these constants could be obtained from similar measurements made in the Mc/sec region where the temperature difference between the maxima would be much larger.

It is seen that the values of $u_\infty-u_0$ and D differ considerably, depending on the method used to obtain them. No single values for these quantities can be given with confidence but in the interest of carrying the analysis somewhat further the following values are proposed:

$$u_\infty-u_0=28 \text{ cm/sec}, \tag{32}$$

$$D=1.5\times10^{-11} \text{ sec °K}. \tag{33}$$

They must be regarded as our conscientious best estimates arrived at by weighing values according to our confidence in them.

In Fig. 17 the attenuation measurements are compared with the LK theory using the values above. A shift of only 1 or 2 μdeg in the position of the λ point

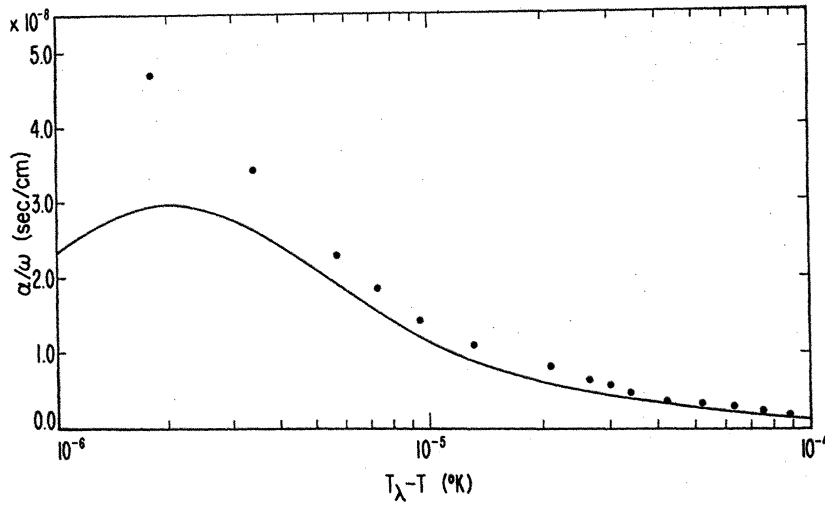

FIG. 17. Comparison of the attenuation at 22 kc/sec to the LK theory. Solid line is theoretical prediction using the averaged values for the LK constants $u_\infty - u_0 = 28$ cm/sec and $D = 1.5 \times 10^{-11}$ sec °K.

would considerably improve the fit to the theory. A similar comparison for the dispersion measurements is is shown in Fig. 18.

The results obtained from attenuation and dispersion measurements can be used to determine the position of the velocity extremum. Using Eq. (18) as the functional form for u_0 and setting the derivative of Eq. (22) to zero yields $f(T_\lambda - T) = g(Z)$, where

$$f(T_\lambda - T) = 2.8 \times 10^{15}/C_p{}^2 + 64.4(T_\lambda - T)^{0.9}, \quad g(Z) = Z^2/(1+Z^2)^2, \tag{34}$$

and Z is again equal to $\omega\tau$. A parametric plot for a frequency of 22 kc/sec is shown in Fig. 19. The curves intersect at two points, 7.2 and 0.5 μdeg below T_λ. As the transition is approached from lower temperatures the increase in velocity due to the relaxation phenomena becomes comparable to the decrease expected from PBFR and a velocity minimum is reached. Closer to the λ point, where $\omega\tau \gg 1$, the rate of increase due to the relaxation effect is greatly reduced, resulting in a velocity maximum. Experimentally, the velocity minimum was found to be about 6 μdeg below T_λ. No velocity maximum was observed although there is an inflection point in the velocity curve very near the λ point. It is interesting to note that the measurements of Chase[7] at 1 Mc/sec also showed no velocity maximum, which should have occurred at about 22 μdeg below T_λ. Chase's measurements were made in an open bath, and this may have precluded its observation.

Because of the hydrostatic head difference the calculated λ points at top and bottom of the resonator differ by 5 μdeg. A recent theoretical result[21] leads to the conclusion that, in the present circumstances,

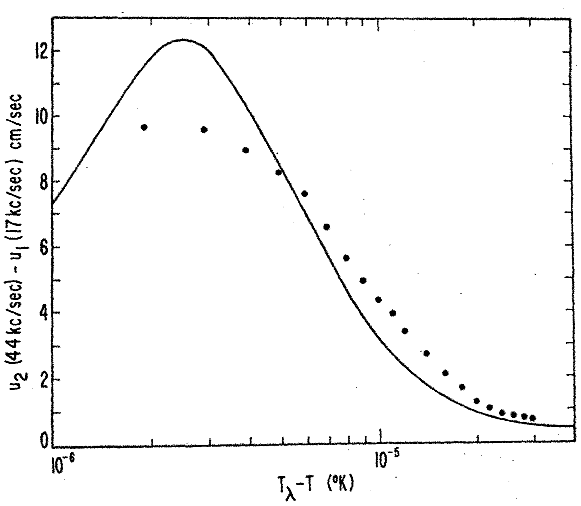

FIG. 18. Comparison of dispersion between the 44 and 17 kc/sec resonances to the LK theory. Solid line is theoretical prediction using averaged values of the LK constants.

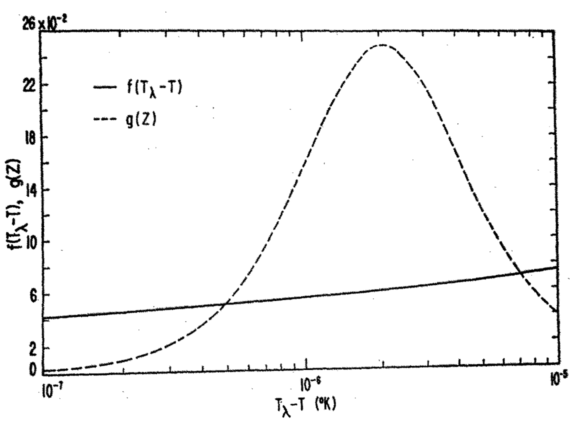

FIG. 19. Parametric plot to determine maximum (at 0.5 μdeg) and minimum (at 7.2 μdeg) in velocity at 22 kc/sec. The functions $f(T_\lambda - T)$ and $g(Z)$ are determined using the averaged values of the LK constants.

[21] L. V. Kiknadze, Tu. G. Mamaladze, and O. D. Cheishvili, Zh. Eksperim. i Teor. Fiz., Pis'ma v Redaktsiyu 3, 305 (1966) [English transl.: Soviet Phys.—JETP Letters 3, 197 (1966)].

liquid helium should be either superfluid throughout or normal throughout. Hohenberg[22] has pointed out that this derivation is based on an incorrect application of the Landau theory. Moreover, recent experiments[23] have revealed the existence of an interface separating the two fluids. If such an interface existed in our resonator this would have had serious effects on the results in the 5-μdeg region, where the interface is traveling through the resonator. None of our observations can be used to directly support the existence of such an interface. On the other hand, such an effect can contribute to the differences between the experimental results and those of the LK theory (or for that matter, any other theory) within approximately 5 μdeg of the λ point.

Ferrell *et al.*[24] have developed a general dynamical scaling theory of the λ transition which predicts a $(T_\lambda - T)^{-1}$ temperature dependence of the attenuation coefficient of first sound below the transition. (No conclusions are reached concerning He-I.) This scaling theory does not employ any adjustable parameter and good agreement[24] is obtained for the absolute magnitude of the attenuation at 22 kc/sec.

2. *He-I*

The attenuation above the transition is plotted against $|T_\lambda - T|^{-1/2}$ in Fig. 20. A linear relationship,

$$\alpha = 1.7\times10^{-5}/(T-T_\lambda)^{1/2}, \qquad (35)$$

is found over a decade in $(T-T_\lambda)$. Because of the difficulty in measuring temperature just above T_λ, the coefficient has an uncertainty of 50%. Chase,[7] using 12.1 Mc/sec, has also observed this temperature dependence over the range 3 to 30 mdeg above T_λ. His values are higher by a ratio of the frequencies raised to the 1.25 power. The attenuation above the transition is less strongly temperature-dependent than below T_λ and does not appear to satisfy a relaxation relation of the form of Eq. (23).

The theories[25–28] which have expanded upon the general approach of LK to account for the attenuation above a second-order phase transition do not predict the temperature dependence found experimentally. Pippard proposed a theory[29] which assumes that above the λ point there could be inclusions of He-II because of fluctuations in temperature. Calculations are difficult because the size and number of inclusions must be

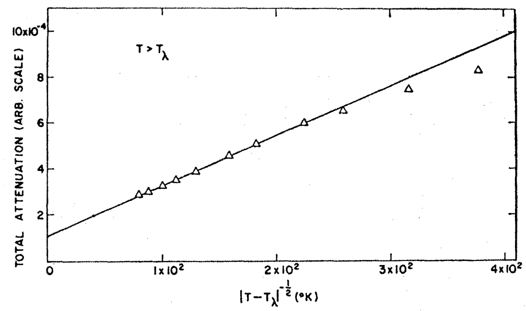

FIG. 20. Total attenuation (arb. scale) versus $|T-T_\lambda|^{-1/2}$. The vertical intercept of the solid line gives the background attenuation above the λ point.

known as a function of temperature. Ferrell *et al.*[30] find a $|T-T_\lambda|^{-1/3}$ singular temperature dependence of the thermal conductivity above the λ point. The attenuation associated with this mechanism is, however, several orders of magnitude below the measured value.

E. Discussion

Recently, Hohenberg has pointed out[31] that many features of the attenuation of first sound may be understood in a very simple way, by extending the dynamic scaling theories.[24,30,32] These theories were originally proposed[30] to explain the attenuation of second sound at the λ point, and later extended to spin-wave modes at magnetic transitions.[32] In both cases one is dealing with what may be called a "critical mode," the mode which dominates the frequency spectrum of the order-parameter fluctuations at long wavelengths near the critical point. For second sound the modification which occurs in the dispersion relation as T approaches T_λ, is of the form

$$\omega_2(k) = u_2 k[1 + iAk\xi + O(k\xi)^2], \qquad (36)$$

where u_2 is the second-sound velocity, A is a constant, and the correlation length ξ diverges as $\epsilon^{-\nu}$ ($\epsilon = |T_\lambda - T|/T_\lambda$). Since it may be shown that $u_2 \sim \epsilon^{\nu/2}$, the damping coefficient D [$D = (2u^3/\omega^2)\alpha$] for second sound is $D_2 \simeq A u_2 \xi \sim \epsilon^{-\nu/2}$, which diverges approximately as the $\frac{1}{3}$ power.[24,30]

Equation (36) may be rewritten as

$$\omega_2(k) = u_2 k[1 + iA\omega_2(k)\tau_2 + O(\omega_2\tau_2)^2], \qquad (37)$$

where the "critical frequency" for second sound is $\tau_2^{-1} \equiv \omega_2(\xi^{-1}) = u_2\xi^{-1} \sim \epsilon$. If it is now assumed that the critical frequency τ_2^{-1} also gives the leading contribution to the damping of first sound, one obtains the formula

$$\omega_1(k) = u_1 k[1 + iB\omega_1(k)\tau_2 + O(\omega_1\tau_2)^2]. \qquad (38)$$

[22] P. C. Hohenberg (private communication).
[23] G. Ahlers (private communication).
[24] R. A. Ferrell, N. Menyhárd, H. Schmidt, F. Schwabl, and P. Szépfalusy (to be published).
[25] I. A. Yakovlev and T. S. Velichkina, Usp. Fiz. Nauk 63, 411 (1957) [English transl.: Advan. Phys. Sci. 63, 552 (1957)].
[26] R. Kikuchi, Ann. Phys. (N. Y.) 10, 127 (1960).
[27] T. Tanaka, P. H. E. Meijer, and J. H. Barry, J. Chem. Phys. 37, 1397 (1962).
[28] A. P. Levanyuk, Zh. Eksperim. i Teor. Fiz. 49, 1304 (1965) [English transl.: Soviet Phys.—JETP 22, 901 (1966)].
[29] A. B. Pippard, Phil. Mag. 42, 1209 (1951).
[30] R. A. Ferrell, N. Menyhárd, H. Schmidt, F. Schwabl, and P. Szépfalusy, Phys. Rev. Letters 18, 891 (1967).
[31] P. C. Hohenberg (private communication).
[32] B. I. Halperin and P. C. Hohenberg, Phys. Rev. Letters 19, 700 (1967).

In this case the damping constant for the noncritical first-sound mode becomes $D_1 = Bu_1^2\tau_2 \sim \epsilon^{-1}$, which yields the observed temperature dependence shown in Fig. 14. Moreover, one would predict a maximum in attenuation at $\omega_1\tau_2 \simeq 1$. Evaluating the formula for τ_2 given above, using the values of Ref. 24, yields $\tau_2 \simeq (2.2\times 10^{-12}/|T_\lambda - T|)$ sec, which is within an order of magnitude of the experimental value [Eq. (33)].

For the critical mode the damping corrections can be expressed either as in Eq. (36) or as in Eq. (37), but for the noncritical first-sound mode the form analogous to Eq. (36), namely,

$$\omega_1(k) = u_1 k[1 + iA'k\xi + O(k\xi)^2], \qquad (39)$$

would predict $D_1 \sim \epsilon^{-2/3}$, which is contrary to observation. It is thus seen that the assumption of the original dynamic scaling theory [Eq. (36)] applies only to the critical modes and must be modified in discussing other modes, as in Eq. (38). While this modification yields good agreement for the attenuation in He-II, it would predict the same behavior in He-I, namely, $D_1 \sim \epsilon^{-1}$, and this is contrary to observation. This discrepancy shows that the point of view adopted here cannot be completely correct, and it is very difficult to see how the observed asymmetry can be reconciled with any of the present scaling ideas.

It is interesting to note that similar arguments reproduce the main features of a recent calculation[33] of sound damping at the liquid-gas critical point. In this case the "critical mode" is a thermal conduction mode whose frequency is $\omega_T = D_T k^2$ and $D_T = \kappa/\rho C_p$, where κ is the thermal conductivity. It is known experimentally[34] that D_T vanishes with an exponent which, although uncertain at the moment, is approximately $\frac{2}{3}$. The sound mode may again be considered noncritical since its contribution to the order-parameter correlation function is smaller (by a factor of order $\epsilon^{1.2}\ln\epsilon$) than the contribution of the critical mode. By introducing the critical frequency $\tau_T^{-1} \equiv D_T\xi^{-2}$, one can again assume a sound dispersion relation of the form given in Eq. (38) (with τ_2 replaced by τ_T). This leads to a sound damping constant $D_s = Au_s^2\xi^2/D_T \sim \epsilon^{-2}$, whose singularity is precisely the one predicted by Kadanoff and Swift.[33]

ACKNOWLEDGMENTS

We would like to thank Dr. P. C. Hohenberg for sharing his theoretical ideas with us and allowing them to be presented in the discussion section. One of the authors wishes to thank Dr. R. Kagiwada for many fruitful discussions. The assistance of R. Williams in some of the experiments is gratefully appreciated.

[33] Leo P. Kadanoff and Jack Swift, Phys. Rev. **166**, 89 (1968); P. C. Hohenberg (private communication).

[34] See, for instance, N. C. Ford and G. B. Benedek, in *Proceedings of the Conference on Phenomena in the Neighborhood of Critical Points* (National Bureau of Standards, Washington, D. C., 1965), p. 150.